

Absence of a spiral magnetic order in Li_2CuO_2 containing one-dimensional CuO_2 ribbon chains

H. J. Xiang, C. Lee, and M.-H. Whangbo*

Department of Chemistry, North Carolina State University, Raleigh, North Carolina 27695-8204, USA

(Received 11 August 2007; revised manuscript received 6 November 2007; published 28 December 2007)

On the basis of first-principles density functional theory electronic structure calculations as well as classical spin analysis, we explored why the magnetic oxide Li_2CuO_2 , consisting of CuO_2 ribbon chains made up of edge-sharing CuO_4 squares, does not exhibit a spiral-magnetic order. Our work shows that, due to the next-nearest-neighbor interchain interactions, the observed collinear magnetic structure becomes only slightly less stable than the spin-spiral ground state and many states become nearly degenerate in energy with the observed collinear structure. This suggests that the collinear magnetic structure of Li_2CuO_2 is a consequence of order by disorder induced by next-nearest-neighbor interchain interactions.

DOI: 10.1103/PhysRevB.76.220411

PACS number(s): 75.10.Pq, 71.70.Gm, 75.10.Hk, 75.25.+z

Copper oxides with CuO_2 ribbon chains made up of edge-sharing CuO_4 squares have one-dimensional chains of spin- $\frac{1}{2}$ Cu^{2+} ions and exhibit unique physical properties. LiCu_2O_2 (Ref. 1) and LiCuVO_4 (Ref. 2) show ferroelectricity when their CuO_2 ribbon chains undergo a spiral-magnetic order at low temperatures. For a chain of spin- $\frac{1}{2}$ ions, a spin-spiral structure is predicted when the nearest-neighbor (NN) ferromagnetic (FM) spin exchange J_1 and the next-nearest-neighbor (NNN) antiferromagnetic (AFM) spin exchange J_2 satisfy the condition $|J_2/J_1| > 0.25$, while an FM structure is predicted if $|J_2/J_1| < 0.25$.³ The copper oxide Li_2CuO_2 (Refs. 4–6) also consists of CuO_2 ribbon chains, but has a different magnetic structure. A neutron powder diffraction study of Li_2CuO_2 at 1.5 K showed a collinear magnetic structure in which the spins of each CuO_2 chain has an FM arrangement with Cu moments perpendicular to the plane of the CuO_2 ribbon and the arrangement between adjacent FM chains is AFM⁷ (hereafter this magnetic structure will be referred to as the AFM-I state). Thus, to explain this collinear magnetic structure, one might expect $|J_2/J_1| < 0.25$ for the CuO_2 chains of Li_2CuO_2 . Indeed, de Graaf *et al.* obtained $|J_2/J_1| = 0.15$ on the basis of first-principles electronic structure calculations using the embedded cluster model.⁸ However, the CuO_2 ribbon chains of Li_2CuO_2 are similar in structure to those of LiCu_2O_2 and LiCuVO_4 , so that $|J_2/J_1| > 0.25$ would have been expected. If $|J_2/J_1| > 0.25$, one needs to ask why a spiral magnetic order does not occur in Li_2CuO_2 . In addition, more than two spin exchange interactions are necessary to describe the magnetic structure of Li_2CuO_2 , and the nature and magnitude of these interactions are not unequivocal.^{9,10} Another puzzle concerning Li_2CuO_2 is that it undergoes a phase transition below ~ 2.4 K to a state believed to be a spin-canted state.^{11–13} So far, the origin and the nature of this phase transition remain unclear.

The spiral magnetic order of LiCu_2O_2 and LiCuVO_4 is a consequence of the spin frustration associated with the NN FM and NNN AFM interactions in their CuO_2 chains. A collinear magnetic order can occur as a consequence of order by disorder,^{14,15} which occurs typically in highly spin-frustrated systems.¹⁶ Provided that a spin-spiral state is the ground state for the CuO_2 chains of Li_2CuO_2 , one might speculate if the AFM-I state of Li_2CuO_2 is close in energy to the spin-spiral state and if Li_2CuO_2 has a large number of

nearly degenerate states around the AFM-I state. In the present work we explore these possibilities by studying the magnetic structure of Li_2CuO_2 on the basis of first-principles density functional theory (DFT) electronic structure calculations and carrying out a classical spin analysis with the spin-exchange parameters deduced from the DFT calculations.

Our DFT electronic structure calculations employed the full-potential augmented-plane-wave plus local-orbital method as implemented in the WIEN2k code.¹⁷ For the exchange-correlation energy functional, the generalized gradient approximation¹⁸ (GGA) was employed¹⁹ with $R_{MT}^{min}K_{max} = 7.0$. To properly describe the strong electron correlation in the 3d transition-metal oxide, the GGA plus on-site repulsion U method (GGA+U) was employed.²⁰ We also examined the energy of Li_2CuO_2 as a function of the magnetic order parameter \mathbf{q} by employing the noncollinear magnetism code WIENncm.²¹

Li_2CuO_2 has a body-centered orthorhombic structure

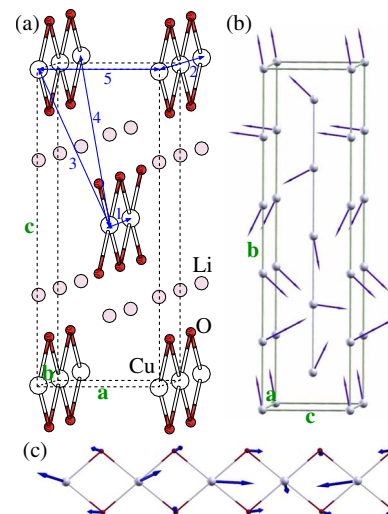


FIG. 1. (Color online) (a) Crystal structure and five spin-exchange paths J_1 – J_5 of Li_2CuO_2 . (b) Cu moments of the spin spiral ground state at $\mathbf{q} = (0, 0.20, 0)$ obtained from the GGA+U noncollinear calculation with $U_{eff} = 6$ eV. (c) Detailed view of the Cu and O moments of a CuO_2 ribbon chain in the spin-spiral ground state shown in (b). For the purpose of illustration, the O moments were increased by 3 times.

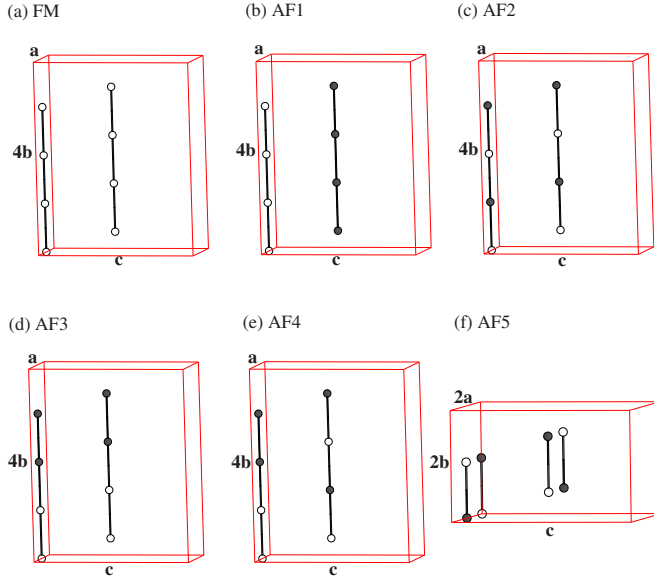


FIG. 2. (Color online) Schematic representations of the six ordered spin arrangements of Li_2CuO_2 employed for GGA+U calculations to extract the five spin-exchange parameters J_1 – J_5 . The solid and open circles represent the up-spin and down-spin Cu sites, respectively.

(space group $Immm$ with $a=3.654$ Å, $b=2.860$ Å, and $c=9.377$ Å),⁷ where the CuO_2 ribbon chains run along the b direction (Fig. 1). As depicted in Fig. 1(a), there are five possible spin-exchange interactions to consider; J_1 and J_2 are NN and NNN intrachain interactions, respectively, and J_3 and J_4 are NN and NNN interchain interactions along the c direction, respectively, while J_5 is the interchain interaction along the a direction. To evaluate the interactions J_1 – J_5 , we calculate the relative energies of the six ordered collinear spin states shown in Fig. 2 in terms of GGA+U calculations. To see the dependence of these spin-exchange interactions on the effective on-site repulsion $U_{\text{eff}}=U-J$, our GGA+U calculations were carried out with U_{eff} ranging from 0 to 10 eV. (For 3d transition metals, U is generally less than 10 eV and the J value is usually 1 eV.) The relative energies of the six ordered spin states of Fig. 2 obtained from our GGA+U calculations are summarized in Table I. Table I shows that the lowest-energy state is the AF3 state when $U_{\text{eff}} \leq 4$ eV, but it is the AF1 state otherwise. In general, the U_{eff} values in the region of 6 eV are most appropriate for Cu-containing

TABLE I. Relative energies per unit cell (in meV) of the various magnetic states with respect to the FM state obtained from GGA+U calculations with different U_{eff} values. There are eight formula units per unit cell (see Fig. 2).

U_{eff} (eV)	0	2	4	6	8	10
$E(\text{AF1})$	-76.72	-46.40	-30.72	-19.04	-11.68	-7.68
$E(\text{AF2})$	5.52	39.12	46.08	46.56	37.60	29.36
$E(\text{AF3})$	-125.12	-64.08	-34.32	-15.68	-5.68	-1.44
$E(\text{AF4})$	-53.28	-8.00	9.84	17.84	17.76	15.04
$E(\text{AF5})$	10.00	40.00	46.16	46.40	37.20	29.20

TABLE II. Calculated exchange parameters (in meV) deduced from GGA+U calculations.

U_{eff} (eV)	0	2	4	6	8	10
J_1	-10.98	-15.58	-15.36	-14.02	-10.86	-8.31
J_2	23.91	15.78	10.44	7.35	4.48	3.00
J_3	1.07	0.34	-0.04	-0.01	-0.09	-0.03
J_4	3.73	2.56	1.95	1.20	0.82	0.51
J_5	-1.12	-0.22	-0.01	0.05	0.09	0.05

magnetic oxides. In terms of the exchange parameters J_1 – J_5 , the energies of the six magnetic states per Cu are written as

$$E(\text{FM}) = (J_1 + J_2 + 4J_3 + 4J_4 + J_5)/4,$$

$$E(\text{AF1}) = (J_1 + J_2 - 4J_3 - 4J_4 + J_5)/4,$$

$$E(\text{AF2}) = (-J_1 + J_2 + J_5)/4,$$

$$E(\text{AF3}) = (-J_2 + 2J_3 - 2J_4 + J_5)/4,$$

$$E(\text{AF4}) = (-J_1 + J_5)/8,$$

$$E(\text{AF5}) = (-J_1 + J_2 - J_5)/8. \quad (1)$$

Thus, by equating the energy differences of these states in terms of the spin-exchange parameters with the corresponding energy differences in terms of the GGA+U calculations, we obtain the values of J_1 – J_5 summarized in Table II, where we employed the convention in which positive and negative numbers represent AFM and FM interactions, respectively. J_5 is very weak in agreement with Mizuno *et al.*¹⁰ The NNN interchain interaction J_4 is much stronger than the NN interchain interaction J_3 , and this finding does not support the assumption by Mizuno *et al.* that J_3 and J_4 are similar.¹⁰ J_4 is stronger than J_3 because the overlap between the magnetic orbitals, which depends on the overlap between the O 2p orbitals of the magnetic orbitals,²² is much more favorable for the path J_4 than for the path J_3 (Fig. 3). The NN intrachain interaction J_1 is FM while the NNN intrachain interac-

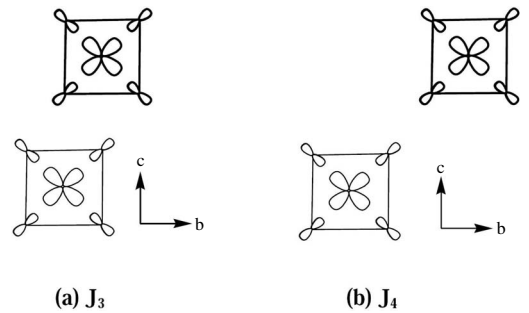


FIG. 3. Arrangements of the CuO_4 squares and their magnetic orbitals associated with (a) the NN interchain interaction J_3 and (b) the NNN interchain interaction J_4 . The two adjacent CuO_2 ribbon chains differ in their a -axis heights by $a/2$. The CuO_4 squares with different a -axis heights are indicated by thick and thin lines.

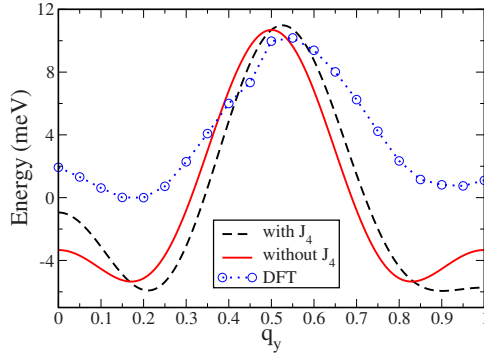


FIG. 4. (Color online) $E(0, q_y, 0)$ vs $(0, q_y, 0)$ relations calculated for Li_2CuO_2 . The solid and dashed lines are based on the classical spin analysis (solid line, only with the intrachain interactions J_1 and J_2 ; dashed line, with the intrachain interactions J_1 and J_2 as well as the interchain interaction J_4). The dotted line is based on noncollinear GGA+U calculations with $U_{\text{eff}}=6$ eV, where the circles represent the calculated points.

tion J_2 is AFM. These intrachain interactions are the same in nature to those reported by de Graaf *et al.*⁸ However, our study shows that $|J_2/J_1| > 0.25$, for all U_{eff} values employed, and hence Li_2CuO_2 should have a spin-spiral ground state as far as isolated CuO_2 ribbon chains are concerned.

To see how the above prediction is affected by the NNN interchain interaction J_4 , we carried out a classical spin analysis based on the Freiser method^{23,24} using the three dominant exchange parameters J_1 , J_2 , and J_4 . The spin interaction energy of an ordered spin state with $\mathbf{q} = (2\pi q_x/a, 2\pi q_y/b, 2\pi q_z/c)$ can be written as

$$\begin{aligned}
 E(\mathbf{q}) = & J_4 \{ \cos[2\pi(q_x/2 + 3q_y/2 + q_z/2)] + \cos[2\pi(-q_x/2 \\
 & + 3q_y/2 + q_z/2)] + \cos[2\pi(q_x/2 - 3q_y/2 + q_z/2)] \\
 & + \cos[2\pi(q_x/2 + 3q_y/2 - q_z/2)] \} + \cos(2\pi q_y) J_1 \\
 & + \cos(4\pi q_y) J_2.
 \end{aligned} \quad (2)$$

For simplicity of our discussion, we will represent \mathbf{q} by (q_x, q_y, q_z) . This $E(\mathbf{q})$ vs \mathbf{q} relation has minima along the $(0, q_y, 0)$ direction. The $E(0, q_y, 0)$ vs $(0, q_y, 0)$ curves calculated with the spin-exchange parameters derived from the GGA+U calculations for $U_{\text{eff}}=6$ eV are presented in Fig. 4. The solid curve, obtained only with the intrachain interactions J_1 and J_2 , shows two minima (at $q_y=0.18$ and $q_y=0.82$) of equal energy. The FM state ($q_y=0.00$) and the AFM-I state ($q_y=1.00$) are identical in energy and are less stable than the two spin-spiral states ($q_y=0.18$ and $q_y=0.82$). These are the expected results in the absence of the interchain interaction because $|J_2/J_1| > 0.25$. The dashed curve, obtained with the intrachain interactions J_1 and J_2 as well as the interchain interaction J_4 , also shows two minima at $q_y=0.21$ and $q_y=0.90$. Note that the interchain interaction J_4 raises the energy of the FM state while lowering that of the AFM-I state. As a result, the $E(0, q_y, 0)$ vs $(0, q_y, 0)$ curve around $q_y=0.21$ becomes sharper while that around $q_y=0.90-1.00$ is nearly flat. Both spin-spiral states are only slightly more stable than the collinear AFM-I state. Our calculations using the spin-exchange parameters obtained with

$U_{\text{eff}} < 6$ eV show that the energy around $q_y=0.21$ becomes lower than that around $q_y=0.90$ and both states have lower energies than the collinear AFM-I state ($q_y=1.00$). In terms of the parameters obtained for $U_{\text{eff}} > 6$ eV, however, the collinear AFM-I state becomes the ground state.

Now we evaluate $E(0, q_y, 0)$ vs $(0, q_y, 0)$ relations on the basis of noncollinear GGA+U electronic structure calculations using the WIENncm code.²¹ In this method, the incommensurate spiral magnetic order is simulated without resorting to the supercell technique by using the generalized Bloch theorem.²⁵ The $E(0, q_y, 0)$ vs $(0, q_y, 0)$ relation calculated for the representative U_{eff} (i.e., 6 eV), presented in Fig. 4 as a dotted line, is quite similar to that found from the classical spin analysis. An important difference is that the noncollinear GGA+U calculations predict the spin-spiral state at $q_y=0.20$ to be slightly more stable than at $q_y=0.95$. The spin arrangement of the spin-spiral state at $q_y=0.20$ is illustrated in Figs. 1(b) and 1(c). In this state of zero total spin moment, the noncollinearity of the spin arrangement occurs not only between Cu spins but also between the O and Cu spins. Our calculations show substantial moments on the O sites, as found in previous studies.^{11,13,26} From our calculation with $U_{\text{eff}}=6.0$ eV, the oxygen spin moment is $0.11\mu_B$, which agrees with the LDA+U result²⁷ and the experimental value (between $0.10\mu_B$ and $0.12\mu_B$).¹³ Our noncollinear GGA+U electronic structure calculations with $U_{\text{eff}} > 6$ eV or with $U_{\text{eff}} < 6$ eV still show that the ground state is a spin-spiral state. Thus, with any reasonable U value, we predict a spin-spiral ground state for Li_2CuO_2 .

From our noncollinear GGA+U calculations, the energy difference between the spin-spiral state at $\mathbf{q}=(0, 0.20, 0)$ and AFM-I state at $\mathbf{q}=(0, 1.00, 0)$ is very small (Fig. 4). In the case of $U_{\text{eff}}=6$ eV, the difference is 1 meV/Cu and decreases with increasing U_{eff} . From the classical spin analysis shown in Fig. 4, this energy difference is even smaller. As already pointed out, the $E(0, q_y, 0)$ vs $(0, q_y, 0)$ curve is sharp around $q_y=0.20$ but nearly flat around $q_y=0.90-1.00$. As a consequence, the states in the region of $q_y=0.90-1.00$ are nearly degenerate and are only slightly less stable than the spin-spiral ground state at $q_y \sim 0.20$; namely, the density of states is much higher in the region of the AFM-I state than around the spin-spiral ground state. The latter provides a natural explanation for why the CuO_2 ribbon chains of Li_2CuO_2 do not exhibit a spiral-magnetic order despite that the CuO_2 chains are very similar in structure to those found in LiCu_2O_2 and LiCuVO_4 , and Li_2CuO_2 has a spin-spiral ground state. In short, the AFM-I structure ($q_y=1.00$) is a collinear order arising from the occupation of many nearly degenerate states around $q_y=0.90-1.10$ and hence is an example of order by disorder.^{14,15} The phase transition below 2.4 K, believed to be a transition to a spin-canted state, might arise from an increased population of the spin-spiral state at $\mathbf{q}=(0, 0.20, 0)$. What distinguishes Li_2CuO_2 from LiCu_2O_2 and LiCuVO_4 is the NNN interchain interaction J_4 , which lowers the energy of the states around the AFM-I state and makes them nearly degenerate.

Our work was supported by the Office of Basic Energy Sciences, Division of Materials Sciences, U.S. Department of Energy, under Grant No. DE-FG02-86ER45259. We thank Dr. D. Dai for useful discussions.

*Corresponding author. mike_whangbo@ncsu.edu

- ¹S. Park, Y. J. Choi, C. L. Zhang, and S-W. Cheong, Phys. Rev. Lett. **98**, 057601 (2007).
- ²Y. Naito, K. Sato, Y. Yasui, Y. Kobayashi, Y. Kobayashi, and M. Sato, J. Phys. Soc. Jpn. **76**, 023708 (2007).
- ³R. Bursill, G. A. Gehring, D. J. J. Farnell, J. B. Parkinson, T. Xiang, and C. Zeng, J. Phys.: Condens. Matter **7**, 8605 (1995).
- ⁴T. Learmonth, C. McGuinness, P.-A. Glans, J. E. Downes, T. Schmitt, L.-C. Duda, J.-H. Guo, F. C. Chou, and K. E. Smith, Europhys. Lett. **79**, 47012 (2007).
- ⁵S.-L. Drechsler, J. Richter, R. Kuzian, J. Mlék, N. Tristan, B. Büchner, A. S. Moskvina, A. A. Gippius, A. Vasiliev, O. Volkova, A. Prokofiev, H. Rakoto, J.-M. Broto, W. Schnelle, M. Schmitt, A. Ormeci, C. Loison, and H. Rosner, J. Magn. Magn. Mater. **316**, 306 (2007).
- ⁶Y.-J. Kim, J. P. Hill, F. C. Chou, D. Casa, T. Gog, and C. T. Venkataraman, Phys. Rev. B **69**, 155105 (2004).
- ⁷F. Sapiña, J. Rodríguez-Carvajal, M. J. Sanchis, R. Ibáñez, A. Beltrán, and D. Beltrán, Solid State Commun. **74**, 779 (1990).
- ⁸C. de Graaf, I. de P. R. Moreira, F. Illas, Ó. Iglesias, and A. Labarta, Phys. Rev. B **66**, 014448 (2002).
- ⁹M. Boehm, S. Coad, B. Roessli, A. Zheludev, M. Zolliker, P. Boni, D. McK. Paul, H. Eisaki, N. Motoyama, and S. Uchida, Europhys. Lett. **43**, 77 (1998).
- ¹⁰Y. Mizuno, T. Tohyama, and S. Maekawa, Phys. Rev. B **60**, 6230 (1999).
- ¹¹U. Staub, B. Roessli, and A. Amato, Physica B **289-290**, 299 (2000).
- ¹²R. J. Ortega, P. J. Jensen, K. V. Rao, F. Sapina, D. Beltran, Z. Iqbal, J. C. Cooley, and J. L. Smith, J. Appl. Phys. **83**, 6542 (1998).
- ¹³E. M. L. Chung, G. J. McIntyre, D. M. Paul, G. Balakrishnan, and M. R. Lees, Phys. Rev. B **68**, 144410 (2003).
- ¹⁴D. Bergman, J. Alicea, E. Gull, S. Trebst, and L. Balents, Nat. Phys. **3**, 487 (2007).
- ¹⁵J. Villain, R. Bidaux, J. P. Carton, and R. Conte, J. Phys. (Paris) **41**, 1263 (1980).
- ¹⁶J. E. Greedan, J. Mater. Chem. **11**, 37 (2001).
- ¹⁷P. Blaha, K. Schwarz, G. Madsen, D. Kvasnicka, and J. Luitz, in *WIEN2K, An Augmented Plane Wave Plus Local Orbitals Program for Calculating Crystal Properties*, edited by K. Schwarz (Technical Universität Wien, Austria, 2001).
- ¹⁸J. P. Perdew, K. Burke, and M. Ernzerhof, Phys. Rev. Lett. **77**, 3865 (1996).
- ¹⁹Our LDA calculations give qualitatively similar results.
- ²⁰V. I. Anisimov, I. V. Solovyev, M. A. Korotin, M. T. Czyżyk, and G. A. Sawatzky, Phys. Rev. B **48**, 16929 (1993).
- ²¹R. Laskowski, G. K. H. Madsen, P. Blaha, and K. Schwarz, Phys. Rev. B **69**, 140408(R) (2004).
- ²²M.-H. Whangbo, H.-J. Koo, and D. Dai, J. Solid State Chem. **176**, 417 (2003).
- ²³M. J. Freiser, Phys. Rev. **123**, 2003 (1961).
- ²⁴D. Dai, H.-J. Koo, and M.-H. Whangbo, Inorg. Chem. **43**, 4026 (2004).
- ²⁵L. M. Sandratskii, Adv. Phys. **47**, 91 (1998).
- ²⁶R. Weht and W. E. Pickett, Phys. Rev. Lett. **81**, 2502 (1998).
- ²⁷D. Mertz, R. Hayn, I. Opahle, and H. Rosner, Phys. Rev. B **72**, 085133 (2005).